Catalytic Partial Oxidation Reformation of Diesel, Gasoline, and Natural Gas for Use in Low Temperature Combustion Engines

Deivanayagam Hariharan[a]; Ruinan Yang[a]; Yingcong Zhou[a]; Brian Gainey[a]; Sotirios Mamalis[a]; Robyn E Smith[b]; Michael A Lugo-Pimentel[b]; Marco J Castaldi[b]; Rajinder Gill[c]; Andrew Davis[c]; Dean Modroukas[d]; Benjamin Lawler[a]

[a]Stony Brook University
[b]The City College of New York
[c]Alloy Surfaces
[d]Innoveering LLC

Abstract

Onboard reforming has relevance to both conventional and advanced combustion concepts. Most recently, onboard reforming has been proposed to enable "Single-Fuel RCCI" combustion and therefore, this paper explores catalytic partial oxidation reforming of three potential transportation-relevant fuels: gasoline, diesel, and natural gas. Reformation is performed at two pressure levels (between 15 to 60 psig) for each parent fuel for equivalence ratios ranging from 3.7 to 7.6 and the gaseous reformate mixtures are characterized with gas chromatography. The percentage of diesel oxidized during reformation is similar across all of the equivalence ratios. However, the percentage of gasoline and natural gas oxidized during reformation decreased with increasing equivalence ratio. The energy released during the reformation process is also calculated and presented for each gaseous reformate fuel. The lower heating value of every reformate fuel is lower than 20% of their respective parent fuel, due to the high concentration of inert gases (mostly nitrogen) in the reformate fuel mixtures.

Two reformed fuels for each parent fuel were then selected to study their autoignition characteristics using HCCI combustion on a Co-operative Fuel Research (CFR) engine. The equivalence ratio is maintained at 0.31 and the combustion phasing was held constant by varying the intake temperature. Although the equivalence ratio is constant, the input energy from the different reformate fuels is not constant due to the component concentrations in the fuel. The gaseous reformate fuels are then compared to gasoline, natural gas, and the primary reference fuels in HCCI to determine an effective Primary Reference Fuel (PRF) number or effective octane rating for each gaseous reformate fuel. The effective octane rating for the gaseous reformate fuels fell slightly above the PRF number scale at an effective octane number of ~110.

Introduction

Low Temperature Combustion (LTC) strategies have been researched extensively in recent years due to their potential to achieve high thermal efficiencies while producing significantly lower NOx and soot emissions compared to conventional combustion modes [1 - 7]. Although they have the aforementioned advantages, most LTC strategies, such as Homogeneous Charge Compression Ignition (HCCI) or Premixed Charge Compression Ignition (PCCI), also have drawbacks; namely, the lack of a direct control over combustion. To address this issue, Reactivity Controlled Compression Ignition (RCCI) was introduced. In RCCI, a low reactivity fuel is premixed with air while a high reactivity fuel is direct injected into the combustion chamber during the compression stroke, introducing a reactivity gradient within the combustion chamber. Combustion can be directly controlled by varying the ratio of the two

fuels and/or adjusting the injection timing of the high reactivity fuel [8 - 10]. In RCCI, gasoline and diesel are the most commonly used low and high reactivity fuels, respectively. Although RCCI addresses the issue of combustion control, the requirement of two separate fuel systems is a significant shortcoming. This has led to a specific adaptation technology – "single-fuel RCCI" where the potential to enable RCCI combustion from a single parent fuel is being investigated.

One example of single-fuel RCCI uses a cetane improver to create two fuel streams from a single parent fuel in the tank. The parent fuel is used as the low reactively fuel. Then, the cetane improver is added to a portion of the parent fuel so that it can be used as a high reactivity fuel as well [11]. Due to the high volatility of gasoline, the direct injection pressure requirement of the high reactivity reduced by 50%. The thermal efficiency and exhaust emission levels were similar to conventional dual-fuel RCCI, and the emissions met EPA HD 2010 emissions mandates without aftertreatment. The compression work was decreased due to the decrease in the low-temperature heat release. With only a small amount of cetane improver, a sufficient difference in the fuel reactivity was achieved, enabling RCCI combustion from a single main fuel tank.

However, using a cetane improver to enable single-fuel has specific disadvantages. First, the cetane improver is essentially a second fuel. The goal is that the cetane improver could be refilled at oil change intervals, similar to diesel exhaust fluid, which is an improvement over conventional dual-fuel RCCI. But the requirement of refilling a separate tank may be a challenge for consumers. Additionally, ethyl-hexyl nitrate (EHN) is the most common and most effective cetane improver. However, EHN is not stable at temperatures over 140 °C as it starts to decompose [12] and therefore presents a challenge for storing EHN in a vehicle application. Additionally, EHN has a fuel-bound NOx group. Therefore, the NOx formed from the CNO group linearly increase with the amount of EHN used [13, 14], which is a significant disadvantage for a low NOx combustion strategy.

Rather than using a cetane improver with a single parent fuel, "single-fuel RCCI" can be enabled from a single parent fuel with onboard fuel reformation [15]. In this variant of single-fuel RCCI, a branch of the fuel stream would be fed to the engine unaltered, while a separate branch of the fuel stream would be reformed using an onboard fuel reformer. The fuel reformer would react the parent fuel, changing its composition, and creating a new fuel stream whose chemical composition and autoignition properties are distinct from the parent fuel. The new gaseous fuel stream is called *reformate*. With the parent fuel and the reformate, it is possible to enable single-fuel RCCI through onboard fuel reformation. However, the composition, properties, and energy balance of the fuel reformer needs to be precisely quantified. This concept is very attractive due to its ability to enable RCCI combustion from a single parent fuel and therefore is a new, active topic of research. For example, Geng et al. used an optical engine with n-heptane as the parent fuel and an online online gas chromatograph to investigate single-fuel RCCI with low temperature reforming [16]. This paper aims to provide new knowledge concerning the reforming process and the reformate mixtures that are produced through the catalytic partial oxidation of diesel, gasoline, and natural gas, as they relate to onboard reforming strategies for transportation applications.

Onboard fuel reformation for transportation applications has been a research topic of interest in the past in a variety of embodiments. Researchers have studied on-board fuel reforming strategy to optimize CI engines by producing hydrogen on-board [17 – 20]. Generally, onboard fuel reforming strategies can be classified as in-cylinder reformation or external reforming. In-cylinder reforming is achieved through partial oxidation (i.e., the products of rich combustion). Examples include Dedicated EGR (D-EGR), and negative valve overlap (NVO) fuel injection in HCCI.

D-EGR achieves onboard fuel reforming using a multicylinder spark ignition (SI) engine where one of the cylinders is dedicated to the reformation process, using rich fuel-air mixtures to partially oxidize the fuel and produce products of rich combustion (i.e., CO and H_2) [21]. A mixture of CO and H_2 is often referred to as *syngas*, although the specific mixture concentrations of syngas can vary widely. The exhaust gas from the reforming cylinder (i.e., the CO and H_2 produced through rich combustion) is recirculated to the intake manifold of the remaining cylinders of the multicylinder engine. This has been shown to improve the overall efficiency by up to 10%, in addition to significantly lowering the engine exhaust emission levels [21, 22].

NVO fuel injection in an HCCI engine cycle is another example of an in-cylinder reforming method that has been researched in the literature [23 – 27]. The results suggest that combustion phasing can be controlled by varying the degree of NVO fuel reformation (for example, by advancing the injection timing during the NVO period [23]). With a split injection strategy, the same effect on the main combustion can be seen by increasing the fraction of fuel injected during the NVO period. High loads require a lower fraction of fuel injected during the NVO period [27].

External, catalytic fuel reforming, where the parent fuel is reacted to produce a mixture of H_2, CO, and other partially reacted hydrocarbon species, can include varying chemical processes [28, 29]. This concept extends the success of fuel reforming for gas turbine combustion applications [30, 31]. The three main mechanisms for external catalytic fuel reforming are steam reforming (SR, also called steam methane reforming, SMR), partial oxidation (POX, or catalytic partial oxidation, CPOX), and auto-thermal reforming (ATR) [32]. Steam reforming is a highly efficient, endothermic method with a long start-up time, where methane and steam are reacted over a catalyst to form CO and H_2. The system is well-suited to run for long periods at steady state [33, 34]. Partial oxidation is an exothermic reaction used to convert hydrocarbon fuels into a mixture of hydrogen, carbon monoxide, and other partially oxidized species. The operating temperature ranges between 1100℃ and 1200℃ to avoid coking in the reactor [27]. POX is compact and has a faster startup than steam reforming [33, 35, 36]. Auto-thermal reforming pairs partial oxidation and steam reforming. Thus, the process is neither exothermic nor endothermic. The ratio of hydrogen to carbon monoxide in the reformed fuel produced from ATR is close to 2, which is higher than what is produced from POX alone [37]. The operating temperature for ATR ranges between 900℃ and 1150℃, depending somewhat on the type of catalyst and the fuel that is used [38 – 41].

Advantages of running a conventional fueled engine with varying hydrogen content in the fuel have been well documented [42, 43]. Bell and Gupta [44] have done an extensive review of prior work with hydrogen-supplemented feeds and have also reported their experience with hydrogen additions of 5, 10 and 15% to a natural gas-fueled spark ignition (SI) engine. NOx emissions as low as 0.15 g/kW-hr were reported over a relatively broad range of equivalence ratios along with associated reduction in CO and HC. The reason for reduced NOx emissions is primarily the lower in-cylinder temperatures due to leaner operation made possible by the much faster flame speeds associated with hydrogen. Improved torque characteristics were also observed with increasing H_2 concentration due to a more advantageous spark timing. It is anticipated that 15–30% of H_2 in the fuel (for gasoline, this amounts to pre-converting ~ 3% of the total fuel) should result in considerable improvement in lean limit stability and consequently result in a significant reduction of NOx, CO and HC emissions [45].

Different types of reforming devices have been developed. For instance, Heywood, et al [46] have been developing a plasma-assisted H_2 generation device (Plasmatron), which has shown greater than 80% NOx reduction in a gasoline-fueled SI engine with potentially increased engine efficiency. Other work by Hydrogen Consultants, Inc. of Littleton, Colorado, has also demonstrated that methane blended with only 5% hydrogen (Hythane®) can result in NOx and CO reduction of up to 50%. Work at Sandia's Combustion Research Facility [47] has identified that "The development of H_2 and H_2-

blended hydrocarbon fuels will boost the use of alternative fuels and lead to cleaner burning turbines."

While the advantages of H_2-spiking of the fuel are numerous, the major hurdle is in demonstrating a feasible and practical means of making H_2 available without compromising system efficiency and/or adequately addressing challenges with control aspects of injecting, mixing and igniting the reactive mixture. Onboard H_2 storage poses uniquely difficult problems. Plasma-assisted devices from Lynntech, Inc. and MIT are plagued by serious efficiency and size penalties and have to overcome significant other hurdles (e.g. electrode corrosion) before they can be considered practical. System efficiency losses should be limited to no more than 1%, and may be offset by improvements in combustion efficiency, higher pressure combustion and/or leaner operation. The reactor is located in the fuel line and analogous to an online fuel filter, located external to the combustor. The proposed concept is to convert part or all of the fuel to H_2 and CO (syngas) via a very compact partial oxidation reactor. The major advantage of this reactor is that it generates the syngas in-line, or in-situ.

In this paper, gasoline, diesel, and natural gas were reformed using a CPOX reaction. The composition of the various gaseous reformate fuel mixtures was determined using gas chromatography, and the energy balance across the reformer is presented. Following that, the combustion characteristics of selected gaseous reformate mixtures are studied individually in HCCI on a CFR engine. The autoignition characteristics of the reformate fuels were then compared to the autoignition of gasoline, natural gas, and the Primary Reference Fuels (PRF) at the same compression ratio and similar intake temperatures to determine an effective PRF number or effective octane rating of the gaseous reformate fuels. The information presented in this paper has relevance to single-fuel RCCI enabled by onboard fuel reforming, or more broadly, to any strategy that involves onboard reforming of gasoline, diesel, or natural gas with a CPOX reaction.

Experimental setup

Experiments were conducted in two separate laboratories. First, the reformation of the three parent fuels was conducted at the Combustion and Catalysis Laboratory at The City College of New York. Second, the combustion characteristics of the reformed gases were studied in detail at Stony Brook University's Advanced Combustion Research Laboratory.

Metallic Monolith Catalyst:

Typically, metallic monolith catalysts are produced by initially applying a high-surface-area-support wash-coat layer directly onto a preformed scaffolding structure followed by the application of the catalytically active material. During this process, the metallic substrates are normally dip-coated or spray-coated with the wash-coat slurry, and excess slurry is removed using an air knife. This can cause a nonuniform distribution of the wash-coat, which promotes hot spot formation within the reactor when used during oxidation and other exothermic reactions. Hot spots can lead to catalyst sintering and even melting of the substrate, thereby reducing catalytic activity. The coating is also weakly adhered to the metal substrate when using this process and therefore the wash-coat is susceptible to physical damage.

In order to overcome these challenges, Alloy Surface Company (ASC) uses a novel approach consisting of "Coat then form" (CTF) catalyst, where the catalyst coating is formed on the surface of a thin metal foil prior to fabrication of the metallic monolith structure. Figure 1 shows a schematic of the formation of an adherent oxide layer, which is inter-diffused into the metal substrate. This oxide layer is more strongly adhered to the metal substrate and has more uniform thickness distribution than a wash-coat layer that is obtained using traditional state-of-the-art spray or dip coating processes as shown in Figure 2.

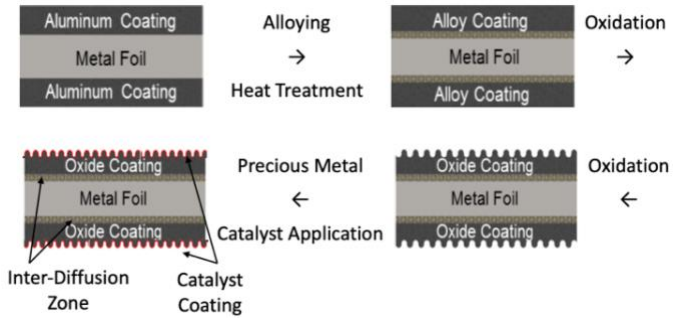

Figure 1: Schematic showing the formation of oxide layer onto metal substrate using ASC proprietary process

Figure 2: The adherent, uniform coating is inter-diffused into the metal substrate with tailored porosity; The ASC coated foil formed into the monolithic geometry chosen for the CPOX tests for this work

ASC-coated foil can be fabricated into various geometries that seek to augment the ratio of geometric surface area to occupied reactor volume as a means of mitigating mass and heat transfer limitations. The coated foil is capable of handling severe stresses during monolith fabrication without causing any spalling. This material is prepared using ASC's continuous web-coating core process, which allows the precise control of coating thickness and uniformity on metal substrates. This coating process can also be applied to a variety of substrates such as stainless steel fibers and tubes to produce high surface area oxide layer with uniform thickness.

Reforming:

A schematic of the experimental setup that was used for the CPOX fuel reformation can be seen in Figure 3.

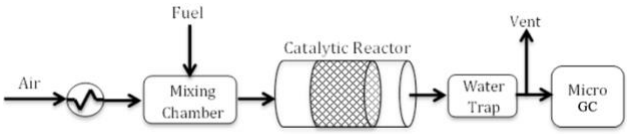

Figure 3: Diagram of the experimental set-up

A catalytic reactor system was built with the capabilities of oxidizing both gaseous and liquid fuels over a catalyst at low and high pressures with simultaneous gas analysis of the reaction products. Natural gas, gasoline, and diesel were reacted at C/O ratios between 0.9 to 2.1. Low- and high-pressure experiments were conducted at 15, 45 and 60 psi, respectively, and reaction temperatures ranged from approximately 850 to 950 °C. At the startup, the catalyst was heated to 500 °C by the reactor furnace shown in Figure 4. The metallic monolith catalyst used in each of these tests is shown in Figure 2. Air and nitrogen were heated to 250 °C and was used to vaporize the fuel in the mixing chamber. Once the reaction began, the reactor furnace was shut off and the reaction was allowed to equilibrate. Water, unreacted liquid fuel, and liquid products were condensed and collected downstream of the reactor. The fuel and air flow rates were adjusted to reach a new C/O ratio while maintaining a gas hourly space velocity (GHSV) between 24,000 and 38,000 /hr.

The product gas was analyzed in real-time using a micro-gas chromatograph (μ-GC). A gas sample was collected concurrently at each reaction condition and analyzed using gas chromatography-mass spectrometry (GCMS). Using both μ-GC and GCMS allowed for detailed quantification of the gas products.

Due to the complexity of the liquid fuels, a quantitative analysis of liquid products via GCMS was not viable and therefore for simplification, the liquid collected was assumed to be water and unreacted fuel. Elemental mass balances based on the gas products were utilized to calculate the composition of liquid products. Using this method, the mass balance was closed with less than 5% error.

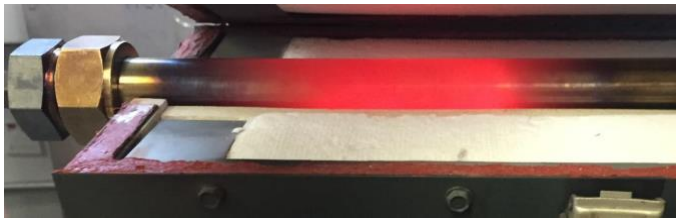

Figure 4: Reactor Furnace

Gasoline, diesel, and natural gas were reformed by a POX process at the pressure conditions described in Table 1. At each pressure condition, the parent fuel was reformed at numerous equivalence ratios to study the effect of equivalence ratio on the oxidation process. The equivalence ratio is the ratio of the actual mass ratio of fuel and air in the mixture to the stoichiometric ratio of fuel and air.

Table 1: Operating condition for three parent fuels tested

	Gasoline	Diesel	Natural Gas
15 psig	✓	✓	✓
45 psig	✓	✓	
60 psig			✓

The reactor furnace temperature was set to 450℃, and the air temperature was increased gradually, using the air heater until the catalyst light-off temperature of 275℃ was reached. All of the heaters were turned off after light-off, as the exothermic reaction is self-sustaining. The mass of fuel calculated based on the target equivalence ratio was introduced into the mixer. This condition was held for 15-30 minutes to ensure stable results, and then measurements are recorded. Next, the injected mass of fuel was varied to reach other desired equivalence ratios. This procedure was repeated for all of the targeted pressure values mentioned in Table 1. The effect of pressure and equivalence ratio on the oxidation process and the energy balance across the reformer is determined by analyzing the product of the reformation process.

Autoignition Characteristics:

The combustion characteristics of the reformed gases were studied on a single cylinder, SI, CFR engine with a side-mounted spark plug. Due to its variable compression ratio capabilities, CFR engines have been extensively used for fuel properties characterization in both conventional combustion modes and advanced combustion modes. Basic engine properties are listed in Table 2; Figure 5 displays the schematic view of the engine.

Although the CFR engine is an SI engine, the combustion mode used throughout this study is HCCI. The spark plug was not used in this study. Instead, the intake temperature is an effective way to control combustion phasing in HCCI; thus, an inline air heater was used to control the temperature of the air entering the engine.

Table 2: Engine parameters

Bore	82.6 mm
Stroke	114.3 mm
Connecting Rod Length	254 mm
Piston pin offset	0 mm
Compression ratio	6:1 to 18:1
Optical Shaft Encoder's Resolutions	0.2 Crank Angle Degrees (CAD)
Intake Valve Opening (IVO)	-350° deg aTDC
Intake Valve Closing (IVC)	-146° deg aTDC
Exhaust Valve Opening (EVO)	140° deg aTDC
Exhaust Valve Closing (EVC)	-345° deg aTDC

The mass flow rate of the intake air is controlled by an MCR Alicat mass flow controller. The gaseous reformate fuels were introduced into the intake plenum, where they mixed with the heated air

to form a homogenous mixture. The gaseous fuels from the tank were regulated to a constant pressure before being introduced to the plenum through another MCR Alicat mass flow controller. A high-speed, water-cooled, Kistler piezoelectric pressure transducer was used to measure the in-cylinder pressure. An encoder, with a resolution of 0.2 CAD, was coupled to the engine's crankshaft. Coolant and oil heaters/radiators were controlled by Omega PID controllers to maintain a constant temperature. All other temperatures, pressures, and flow rates were monitored and controlled by a custom LabVIEW code.

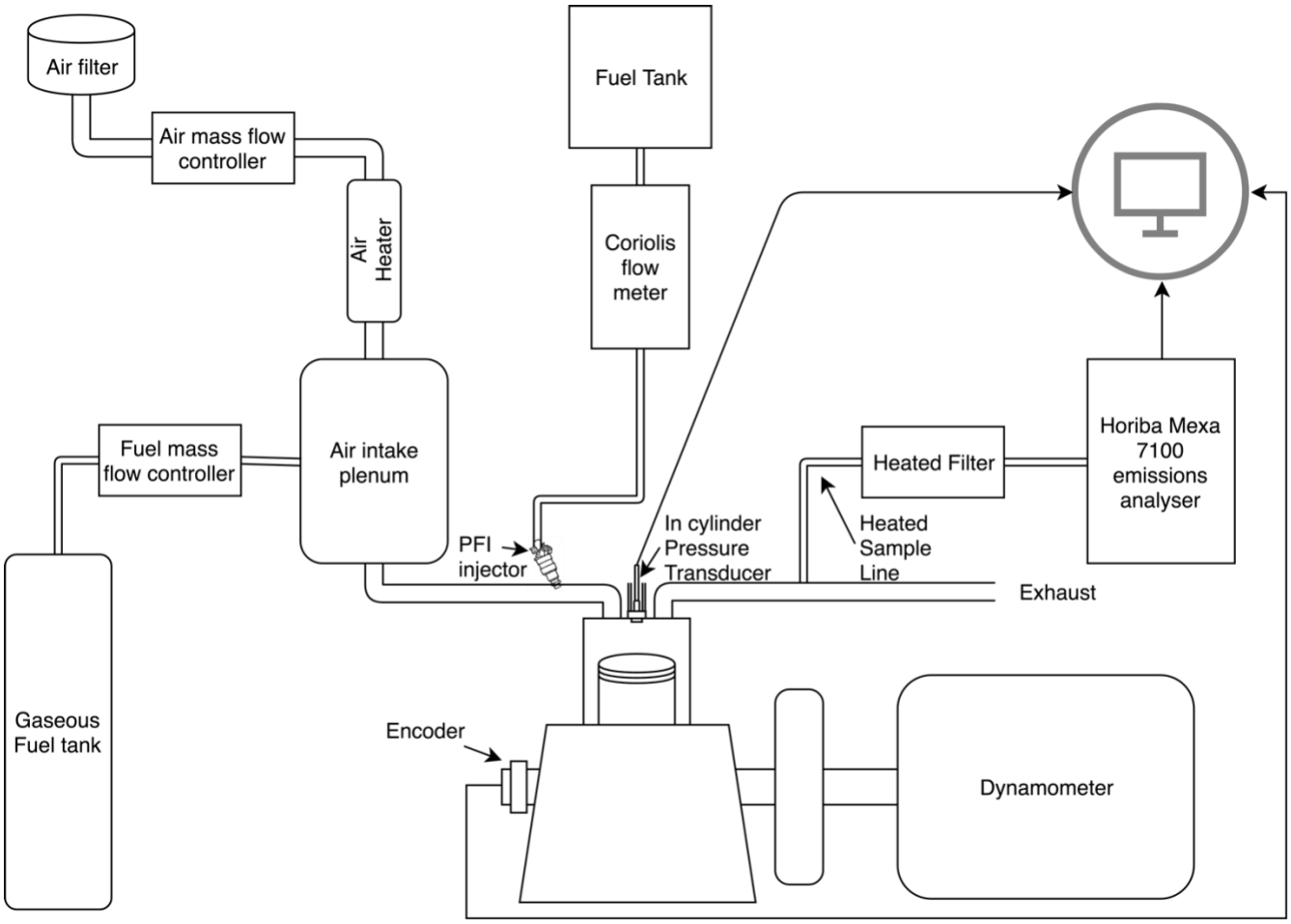

Figure 5: Schematic of the CFR engine

A 30 hp active DC dynamometer was connected to the flywheel of the CFR engine to provide a constant speed of 1200 rpm for all of the data collected. The emissions were measured by a Horiba MEXA-7100 D-EGR motor exhaust gas analyzer. The analyzer measures CO, CO_2, O_2, NOx, CH_4, and total unburned hydrocarbons (THC).

Two characteristic gaseous reformate fuel mixture compositions were chosen for further analysis to be representative of a relatively high degree of reformation and a relatively low degree of reformation. Their autoignition characteristics were studied using HCCI combustion. The experiments were conducted on the CFR engine at a compression ratio of 16 and a constant engine speed of 1200 rpm. The reformate fuels were obtained as gas bottles whose contents were chosen based on the GC results from the reformation process. A thorough

justification of this approximation is provided in the Results section below. The equivalence ratio was maintained at 0.31 and CA50 was maintained at 5 degrees after TDC for every fuel by varying the intake temperature. The Maximum Pressure Rise Rate (MPRR) and Coefficient of Variation (CoV) of Net Indicated Mean Effective Pressure (IMEPn) are limited to 3% and 5 bar/deg, respectively. The heat release characteristics, combustion duration, magnitude of heat transfer losses, efficiency, and exhaust emissions have been analyzed in detail. Finally, based on a previous study of PRF blends [48] and the intake temperature required to autoignite the reformate fuels, an effective PRF number or effective octane rating for the six reformate fuels was determined.

Results and Discussions

All three parent fuels underwent POX at numerous equivalence ratios under two pressure conditions. During the oxidation process, the mass flow rates of the reactants were measured directly. The mass flow rates of products were calculated from the measured mass of each individual component. The percent difference between these two mass flow measurements is called the mass balance. The mass balance is closed within 5%. Table 3 shows a list of every condition tested, with only the major species for each reformate mixture shown. The complete molar concentrations of the products after the reformation process for the six representative cases can be seen in Table A 1. The concentrations of H_2O in Table 3 are calculated because of the requirement for water to be removed prior to gas analysis. For both gasoline and diesel, the results are normalized to exclude the components with a concentration less than 0.1%. The full list of components with their respective concentrations can be seen in Table A 2 in the appendix.

Since the CPOX reaction was used to reform the parent fuel, air was used as an oxidizer. This results in large amount of inert N_2 gas in the reformate. Additionally, although the goal is to produce CO and H_2 from the parent fuel during the reformation process, some amount of fuel underwent complete oxidation to produce CO_2 and H_2O. The inert gases present in the reformate fuel mixture reduce the energy density of the fuel compared with the parent fuels. The effects of pressure and equivalence ratio for each parent fuel were studied in detail along with the energy released during the reformation process.

Additionally, the fuel conversion of natural gas, gasoline, and diesel was monitored throughout each test condition. Mass balances were used to calculate the unreacted fuel during gasoline and diesel experiments, while unreacted natural gas was measured using the μ-GC.

Natural Gas:

The fraction of CH_4 oxidized during the natural gas reformation process is inversely proportional to the equivalence ratio of the fuel-air mixture for both of the pressure conditions. It can be seen in Table 3 that as the equivalence ratio increases, the concentration of methane in the reformate product increases.

Table 3: Molar concentration of the products after the reformation process

		Equivalence ratio	Molar Concentration Out (%)								Energy Released During Reformation
			H_2	O2	N_2	CH_4	CO	CO_2	Fuel	H_2O	
Natural Gas	Low P	7.62	16.8%	0.0%	41.2%	24.0%	7.1%	3.7%	NA	7.3%	19.4%
		6.67	16.4%	0.0%	43.0%	21.6%	7.3%	3.7%	NA	8.0%	19.8%
		6.06	16.7%	0.0%	41.8%	15.6%	7.9%	3.4%	NA	14.7%	30.5%
	High P	6.00	21.0%	1.1%	39.8%	20.4%	10.5%	3.2%	NA	4.0%	6.2%
		5.00	20.6%	1.6%	43.0%	16.4%	10.4%	3.3%	NA	4.6%	9.8%
		4.00	21.2%	2.2%	46.8%	10.3%	11.1%	3.3%	NA	5.0%	17.6%
		3.75	20.9%	2.5%	48.5%	8.4%	11.0%	3.4%	NA	5.3%	22.9%
Gasoline	Low P	6.40	6.4%	0.6%	56.6%	2.8%	5.9%	6.1%	4.5%	11.3%	15.8%
		5.20	7.6%	0.3%	55.7%	3.5%	5.8%	4.6%	3.6%	14.4%	13.7%
		4.80	9.8%	0.1%	55.0%	3.7%	15.0%	3.9%	1.7%	6.9%	22.3%
	High P	5.19	7.2%	0.0%	51.8%	3.5%	9.3%	5.9%	1.8%	16.5%	33.9%
		4.96	3.3%	0.0%	55.0%	2.5%	5.9%	6.9%	2.4%	20.1%	36.5%
		4.91	2.9%	0.9%	55.3%	2.9%	5.0%	6.6%	2.4%	20.0%	35.5%
		4.83	2.9%	0.0%	55.4%	2.6%	5.0%	7.1%	2.2%	20.9%	38.3%
		4.65	3.1%	0.0%	55.2%	2.7%	5.0%	7.2%	2.0%	20.5%	37.2%
Diesel	Low P	5.18	6.6%	0.0%	59.0%	3.0%	8.9%	7.4%	2.0%	7.9%	16.5%
		4.17	2.6%	0.2%	65.5%	1.1%	2.9%	9.3%	2.5%	13.2%	19.7%
		4.15	5.7%	0.0%	60.7%	2.2%	7.4%	6.9%	1.7%	11.4%	17.5%
	High P	5.09	3.4%	0.1%	61.6%	2.6%	5.3%	7.7%	2.6%	12.2%	15.8%
		4.44	3.8%	0.0%	62.0%	2.4%	5.8%	7.7%	2.1%	11.9%	17.3%
		3.67	4.9%	0.0%	62.3%	2.1%	7.2%	7.4%	1.5%	11.4%	21.1%

However, the high-pressure methane conversion rate was lower than the low-pressure methane conversion rate at all equivalence ratios. Furthermore, the formation of CO, which is a product of methane oxidation, is also inversely proportional to the equivalence ratio, due to the fall in the methane conversion rate.

The CPOX of natural gas was performed at C/O ratios from 0.9 to 1.9 at low (15 psi) and high (60 psi) pressures resulting in conversion rates between 31% and 68% as shown in Figure 6. For both pressure conditions, conversion decreases with increasing C/O ratio and begins to taper at higher C/O ratios. For the C/O ratios tested, conversion decreases more drastically with respect to C/O ratio for high-pressure experiments.

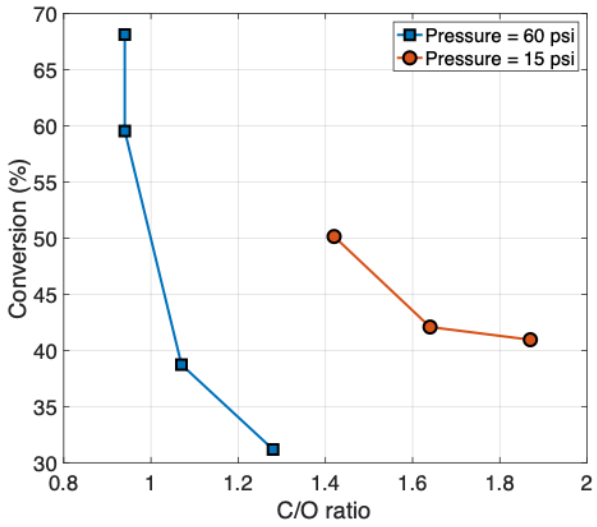

Figure 6: The conversion of natural gas as a function of C/O ratio for high- and low-pressure experiments

Gasoline:

Similar to natural gas, the fraction of gasoline oxidized during the gasoline reformation process is inversely proportional to the equivalence ratio. Referring to Table 3, the molar concentration of gasoline in the reformed product increases with equivalence ratio in the low-pressure reformation, whereas under the high-pressure condition, the molar concentration of unreacted gasoline does not vary with equivalence ratio. The concentration of CO_2 follows the same trend as the fuel, while CO and H_2 follow the opposite trend, since they are formed due to incomplete oxidation of fuel. The conversion rate of gasoline under the high-pressure condition was noticeably higher than the low-pressure condition at a similar equivalence ratio.

The trend similar to natural gas was observed during low-pressure gasoline CPOX tests at C/O ratios changed from 1.5 to 2.1 as shown in Figure 7. However, for high-pressure gasoline CPOX, conversion displayed a parabolic behavior with respect to C/O ratio. From this observation, it can be hypothesized that gasoline conversion during low-pressure CPOX would also increase analogously at higher C/O ratios.

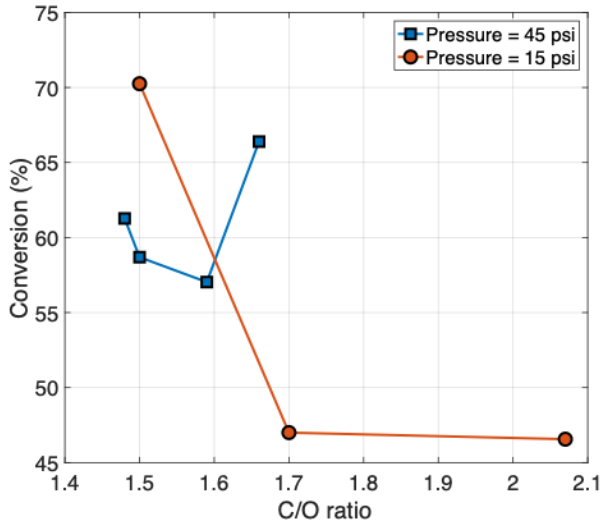

Figure 7: The conversion of gasoline as a function of C/O ratio for high- and low-pressure experiments

Diesel:

In the diesel reformation process, oxidation of the fuel is similar for each of the equivalence ratios for both low- and high-pressure reformation. The fact that diesel fuel exhibits low-temperature heat release could be a reason for the insensitivity to equivalence ratio. Nonetheless, H_2O and CO concentrations were comparatively higher for the high-pressure reformation.

During low-pressure diesel tests, conversion rates were measured at two different GHSV while

holding the C/O ratio constant at 1.1. When increasing the C/O ratio to 1.4, the GHSV also increased slightly. Figure 8 demonstrates the dependence of diesel conversion on with increasing C/O ratio for both low- and high-pressure experiments. Also, conversion is slightly higher during low-pressure tests. These results coincide with the results during natural gas and gasoline tests at C/O ratios below 1.6.

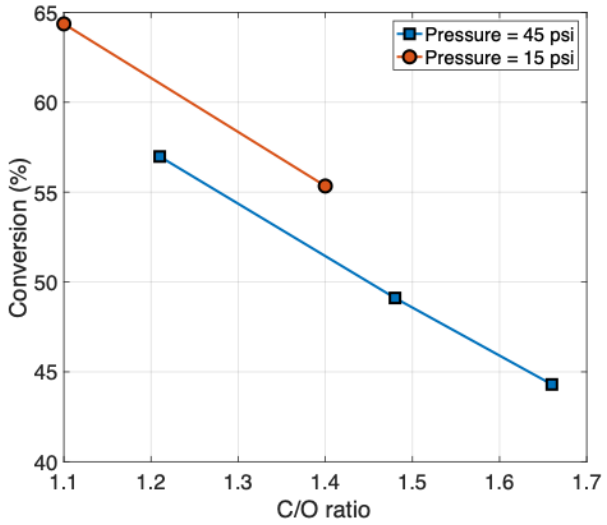

Figure 8: The conversion of diesel as a function of C/O ratio for high- and low-pressure experiments

Energy Balance Over the Reformer:

Since the CPOX reaction is exothermic, the amount of energy released during the reformation process is an important consideration. Although this released energy helps to sustain the high temperatures needed over the catalyst, any energy released in the reformer constitutes a lost opportunity to produce work in the engine and counts against the overall efficiency of the system. The energy lost during the reformation process is calculated based on the molar concentration and the individual lower heating values (LHV) of both the reactants and the products. The energy released during reformation is shown in the final column of Table 3. The total energy lost in the diesel reformation process remains relatively constant, irrespective of the pressure and equivalence ratio, because of the similarity in their product's concentrations. Again, this factor could be due to the significant amount of low-temperature heat release that exists for diesel fuel.

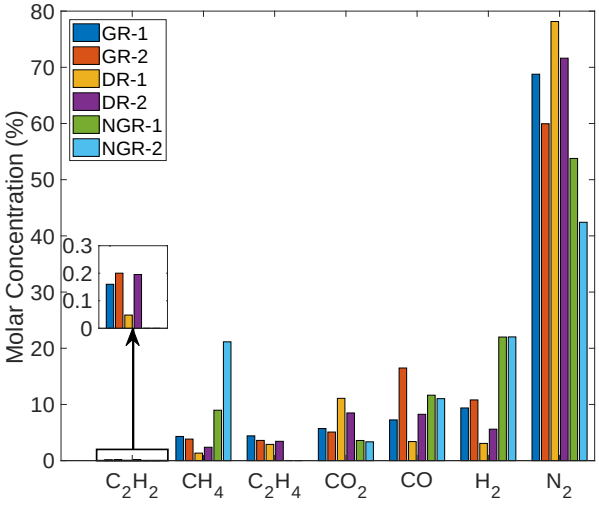

Figure 9: Molar concentrations of reformate fuels

On the other hand, both the natural gas and the gasoline reformation process have a lower percent of energy lost as the equivalence ratio increases, because of their lower conversion rate.

Two characteristic gaseous reformate fuel mixture compositions were chosen for further analysis to be representative of a relatively high degree of reformation and a relatively low degree of reformation. The molar concentrations of the six selected reformate fuels are shown in Figure 9 and their lower heating values have been compared against their parent fuel in Figure 10. The lower heating values of the reformate fuel mixtures are significantly lower than the parent fuel due to the large fraction of inert gases (N_2, CO_2, and H_2O) that result due to the CPOX reaction. The energy density of the fuel plays a vital role in combustion. Due to the use of air in the partial oxidation reaction, the reformate fuel mixtures are diluted with more than 40% inert gases (mostly nitrogen, but including some carbon dioxide and water vapor from complete oxidation). As a result, their LHVs are found to be less than 20% of their corresponding parent fuel's LHV.

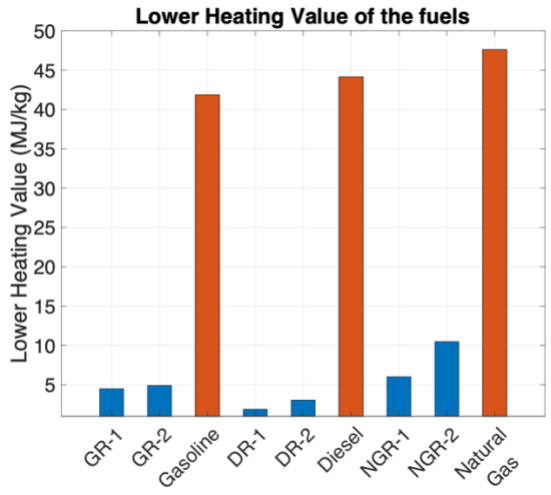

Figure 10: Lower heating value of reformate fuels and their parent fuels

In the next section, the autoignition characteristics from testing six representative reformate fuel mixtures on the CFR engine are shown. In order to test the reformate fuel mixtures in the CFR engine, gas bottles were acquired with a composition of gas species that matched the reformate fuel mixtures as closely as possible. The products of reformation contained a large number of different species with very low concentrations, especially when reforming diesel and gasoline. Additionally, there is some water vapor in the reformate fuel mixture. Therefore, the gas bottles only contained the species whose concentration in the reformate mixture was larger than 1%, with three exceptions. First, any unreacted liquid parent fuel (i.e., gasoline or diesel) cannot be present in the bottle. Second, since acetylene has been shown to play a significant role in the autoignition timing of reformed fuel mixtures [49], the exact concentration of acetylene in the reformate fuel mixture was used in the gas bottles. Third, due to the practical difficulties of having H_2O in gaseous form in the gas bottle, the concentration of the components in the gas bottles were normalized without water.

Due to these factors, the concentrations of species that were tested in the CFR engine do not perfectly match the concentrations that exited the fuel reformer, which creates some uncertainty that the autoignition results will be representative of the gaseous reformate fuel mixture. To test the effects of these slight changes to the autoignition characteristics of the reformate fuel, a single zone, closed cycle simulation was performed with detailed kinetics. The simulation used Cantera to solve the chemical kinetics and used the Lawrence Livermore National Laboratory (LLNL) gasoline surrogate with ethanol mechanism that has 323 species. In the simulation, the experimental composition was first simulated with a combustion phasing that matches the experiments below. Then, the exact reformate mixture composition was simulated to understand the effects of approximating the reformate fuel composition in the gas bottles. The IVC temperature was adjusted to match the combustion phasing of reformate mixture to the experimental composition such that the IVC temperature difference can be a quantitative metric to compare the differences in the autoignition timing of the two slightly different compositions.

The results are shown in Figure 11. The IVC temperature difference between the exact reformate composition and the experimentally tested composition was 1.5 K, which is a negligible difference in their autoignition tendency. This result proves that approximating the fuel composition for the practical constraints of the gas bottle does not significantly affect the autoignition tendency of the gaseous reformate fuel mixture.

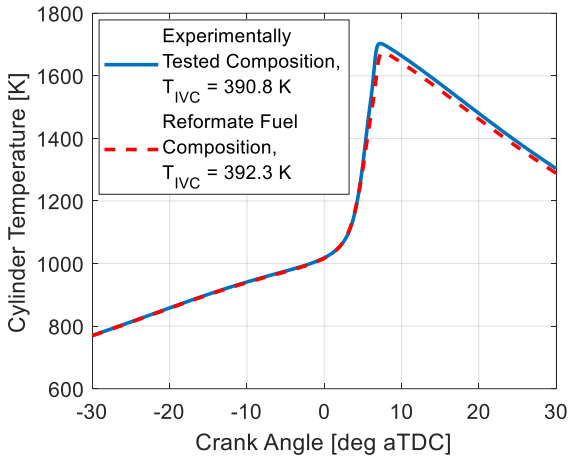

Figure 11: Single zone closed cycle chemical kinetics simulations showing that the experimentally tested compositions has a similar autoignition timing as the reformate fuel mixture composition

Autoignition Characteristics:

The pressure and gross heat release rate (GHRR) for all the reformate fuels are shown in Figure 12 grouped based on their parent fuel.

For a valid comparison, CA50 and equivalence ratio are held constant within one crank angle degree and 0.04, respectively. In Figure 12.a, Gasoline Reformate 2 (GR-2) has a higher peak pressure and peak heat release rate compared to Gasoline Reformate 1 (GR-1). This is because GR-2 has a higher concentration of CO and H_2, and lower concentration of inert gases, like N_2 and CO_2 compared with GR-1. With less inert gases to act as a heat sink, and more reactive components, such as CO and H_2, the amount of heat release produced from GR-2 is higher than GR-1. To have identical combustion phasing, GR-1 requires a higher intake temperature than GR-2.

Comparing the components of Diesel Reformate 1 (DR-1) and Diesel Reformate 2 (DR-2), the biggest differences are in the concentration of CO and N_2, similar to the gasoline reformates. Additionally, DR-2 has a lower amount of CO_2 and a higher amount of H_2 than DR-1. Since the fuel properties are very similar to the gasoline reformates, the trends of pressure and heat release are the same.

In Figure 12.c, the pressure and heat release rate of the two natural gas reformates are compared. From Figure 9, it can be seen that the biggest concentration difference between the natural gas reformates is the concentration of CH_4. With CH_4 being a high-octane component, as the concentration of CH_4 changes from 9% to 21%, the required intake temperature to autoignite the reformate fuel increases. Natural Gas Reformate 2 (NGR-2) required a 12% higher intake temperature than Natural Gas Reformate 1 (NGR-1) due to the difference in methane concentration. The influence of the higher intake temperature on NGR-2 can be seen in ratio of specific heats during the compression (Figure 13.c).

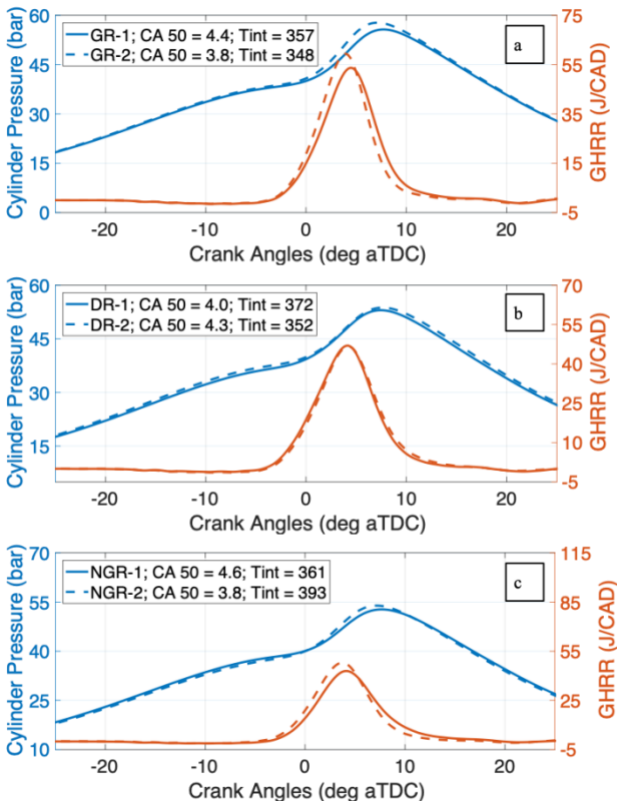

Figure 12: Pressure and GHRR of the reformates of a) gasoline, b) diesel, and c) natural gas

Figure 12 shows the ratio of specific heats for the six reformate fuels grouped by their parent fuel. The ratio of specific heats, commonly known as γ, is a crucial parameter that determines the pressure during the compression stroke and plays a major role in the efficiency of the thermodynamic cycle. The

ratio of specific heats is a strong function of the temperature and the molecular structure of the gas constituents. The ratio of specific heats for any single molecule depends on the number of degrees of freedom in which that molecule can store energy. Monatomic molecules, which have only three degrees of freedom to store energy, have the highest ratio of specific heats. Larger molecules have more degrees of freedom which decreases the ratio of specific heats. Further, increasing the temperature of molecules will "unfreeze" certain vibrational degrees of freedom for polyatomic molecules, which also lowers the ratio of specific heats.

Figure 13.a show that the ratio of specific heats of GR-2 is higher throughout the compression process due to the 3% lower intake temperature. The trend is same for both the diesel reformates (Figure 13.b) and the natural gas reformates (Figure 13.c); with the higher intake temperature, the ratio of specific heats during the compression process decreases by up to 0.01.

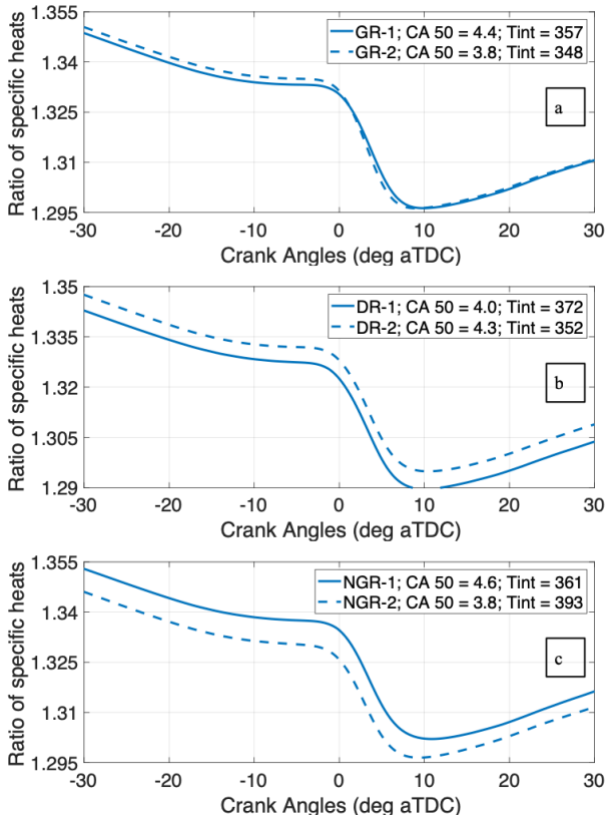

Figure 13: Ratio of specific heats of the reformates of a) gasoline, b) diesel, and c) natural gas

An interesting finding that is shown in Figure 12 is that the heat release characteristics are single-stage and very similar to other conventional fuels in HCCI. With the large mixture of various species, it was unclear if the heat release characteristics would have any unique features. However, Figure 12 shows that the heat release characteristics do not have any unique features and are instead very similar to conventional fuels. To explore the heat release characteristics in more detail and perform a more quantitative comparison, Figure 14 shows the heat release rate of one of the six gaseous reformate fuels compared with HCCI of iso-octane at same equivalence ratio and compression ratio. All of the gaseous reformates, unlike some of the parent fuels, exhibit a single stage heat release process (Figure 12). When the combustion phasing is constant, irrespective of the reformate fuel and its specific composition, the heat release characteristics are very comparable to iso-octane (PRF 100) as a reference.

This result shows that although there are a wide variety of different components in every fuel, the combustion process is not dictated by any individual component; it is always the combined effect. Since the gaseous reformate fuel mixture resulted from a partial oxidation process of a given parent fuel, the species in the mixture are combustion intermediates for that particulate fuel. As a result, the HCCI heat release characteristics are very similar to other conventional fuels.

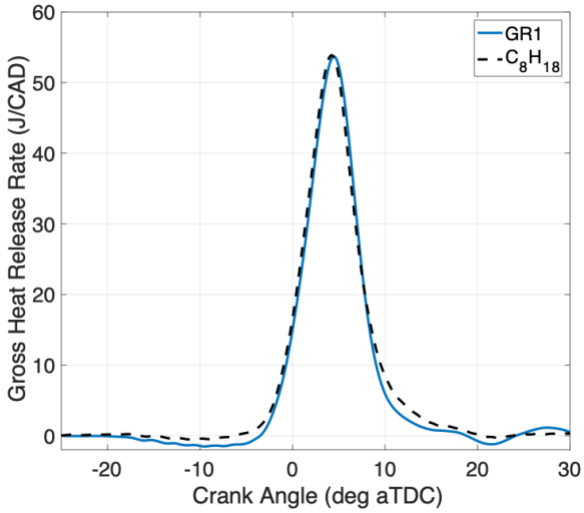

Figure 14: Similarity in the heat release characteristics of an example gaseous reformate fuel and iso-octane

The combustion duration is calculated based on two different ranges, namely CA25to75 and CA10to90. Due to the absence of a two-stage heat release, the combustion duration CA10to90 will not be affected by any low-temperature heat release. Therefore, the combustion durations, CA25to75 and CA10to90, follow the same trend, shown in Figure 15. Although the components of the fuel change, the combustion duration remained constant (within 1 CAD and 2 CAD for CA25to75 and CA10to90, respectively). This is a result of the constant combustion phasing and equivalence ratio used. Also, the combustion duration of all six gaseous fuel reformates were compared with HCCI combustion of two liquid fuels, iso-octane and gasoline. Iso-octane and gasoline are chosen as reference liquid fuels as their reactivity is close to the gaseous reformate fuels.

The gaseous reformate fuel mixtures have a similar burn duration compared to the conventional liquid fuels.

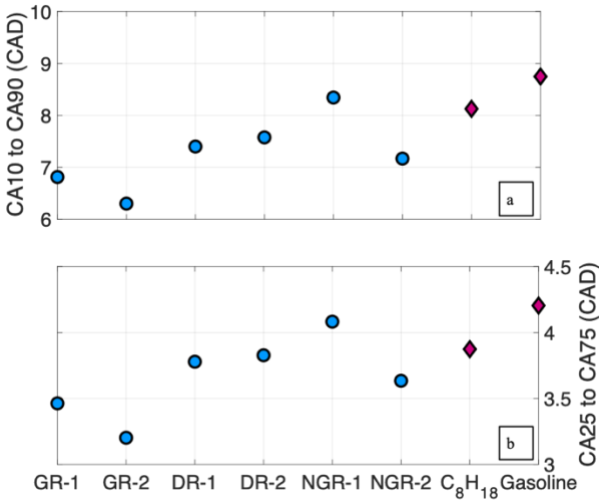

Figure 15: a) CA10to90 and b) CA25to75 combustion duration

Even though the compression ratio, equivalence ratio, and engine speed are constant, the trapped mass changes somewhat due to the change in the volumetric density causes by differences in the intake temperature. The density of air changes due to the differences in the intake temperature. Additionally, since the composition of the fuel changes, the mass flow rate of fuel changes for the different gaseous reformate fuels to maintain a constant equivalence ratio. The density of each gaseous reformate fuel can be seen in Table A 2.

At the constant compression ratio and equivalence ratio, the combustion phasing was directly controlled by the intake temperature. Even though the equivalence ratio was maintained at 0.31, the chemical energy in the incoming fuel mixture ("Energy In") was different due to the difference in fuel composition and the trapped mass. With the calculated lower heating value and the measured mass of fuel (Table A 2), the "energy in" is calculated and reported in the Figure 16, along with the IMEPn and thermal efficiency.

The total amount of heat released during combustion process is directly proportional to the

combustion efficiency and the energy in. Since the combustion efficiency is similar across all of the gaseous reformate fuels (Table A 2), the IMEPn for each reformate follows the same trend as energy in, for both gasoline and diesel reformates (Figure 16). The energy in for the liquid fuel is slightly higher than the gaseous reformate fuels due to the liquid fuels having a lower required intake temperature to maintain combustion phasing, which increases the incoming charge density.

The thermal efficiency was similar all of the reformate fuels tested and both of the reference liquid fuels. Previous work showed that the thermal efficiency in HCCI is sensitive to the intake temperature because of the impacts on volumetric efficiency [48]. The differences in thermal efficiency in Figure 16 can be explained by the intake temperature differences. The two natural gas reformates and DR-1 reached lower IMEPn due to their higher required intake temperatures. With the higher intake temperature, the intake air was less dense, which reduces the trapped mass in the cylinder. Additionally, higher intake temperatures lead to higher peak temperatures resulting in higher heat transfer losses.

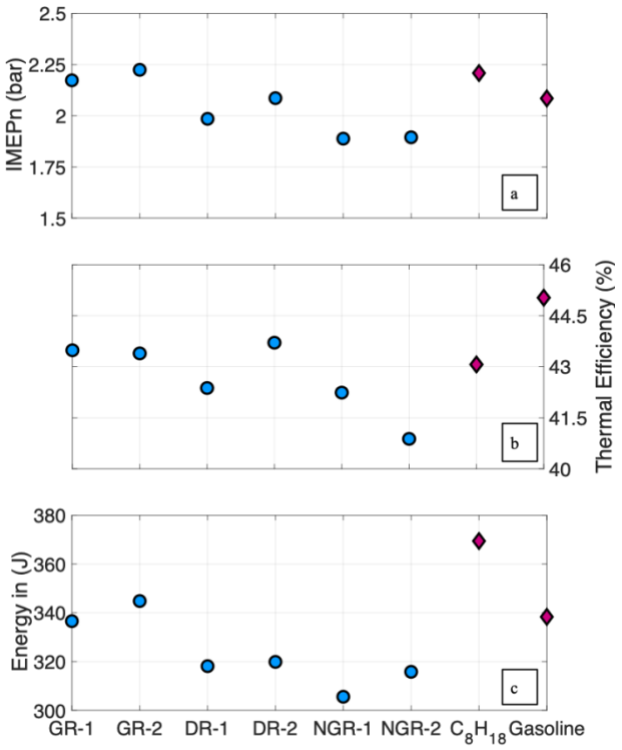

Figure 16: a) Net indicated mean effective pressure (IMEPn), b) thermal efficiency, and c) chemical energy in the fuel mixture

The heat transfer losses are proportional to the bulk temperature. Figure 17 shows the instantaneous bulk temperature and the heat loss calculated using the modified Woschni heat transfer correlation [50]. It can be seen that the heat loss follows the same trend as the bulk temperature for all the six reformate gaseous fuels. The peak bulk temperature itself depends on the amount of inert gases in the cylinder, since the inert gases act as a heat sink. With the difference in the energy in and the inert gas concentration across different fuels, the bulk temperature after compression changes for different fuels. The actual values are tabulated on Table A 2.

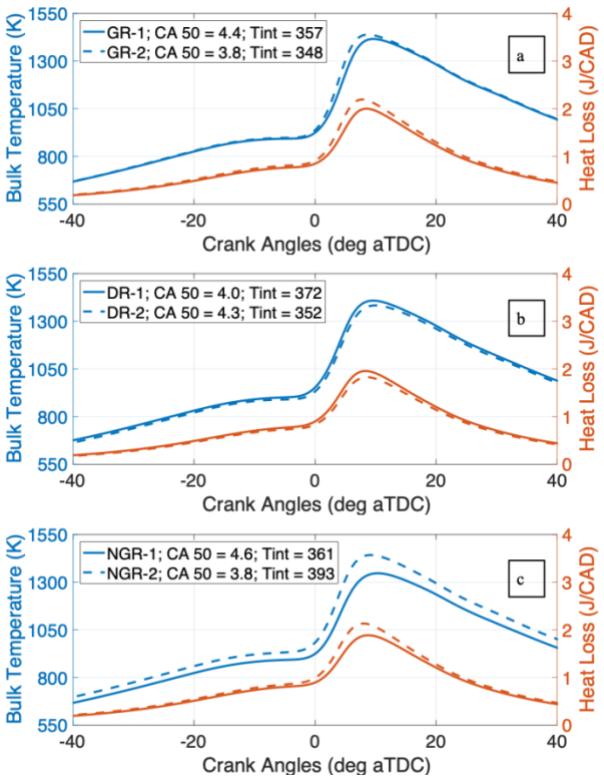

Figure 17: Bulk temperature and heat loss of the reformates of a) gasoline, b) diesel, and c) natural gas

Figure 18 shows the Indicated Specific (IS) CO, CO_2, THC, and NOx. Indicated specific emissions are presented instead of the emission index because the mass flow rates of the gaseous and liquid fuels were drastically different due to the difference in their volumetric and energy densities. LTC attempts to produce near-zero NOx emissions by keeping in-cylinder temperatures below the NOx production threshold. The maximum ISNOx of 0.04 g/kW-h is lower than any conventional combustion mode [51], because of the low peak bulk temperatures. The ISTHC emissions in Figure 18.a are related to the peak bulk temperature. The ISTHC emissions of the diesel reformates are high due to their lower bulk temperature compared with other fuels at the same combustion phasing. For liquid fuels, the combustion efficiency was slightly lower than the gaseous fuels, which results in higher THC emissions.

Along with THC and NOx emissions, CO and CO_2 emissions were also measured using the Horiba Mexa-7100 D-EGR. During combustion, CO_2 is normally formed by oxidation of CO; this oxidation diminishes at temperatures below 1500K [52]. The fuel itself, however, has a CO_2 concentration of up to 10%. CO_2 emissions are thus dictated by both the CO_2 concentration in the fuel and the in-cylinder temperature to oxidize the CO into CO_2. Usually CO emissions are formed due to incomplete combustion. However, in this case, the gaseous fuel mixture is a partially oxidized fuel. Therefore, a portion of the fuel is CO, which means that the CO emissions in the exhaust are due to both incomplete combustion of hydrocarbons in the reformate fuel and the CO concentration itself in the reformate fuel. From Table A 2 , it can be seen that the peak bulk temperature was always lower than 1500K for all the reformate gaseous fuels. Figure 18.b shows the ISCO for both gasoline and diesel reformate mixtures follows the same trend as the CO concentration in the reformate fuel. Similarly, as CO increases, the $ISCO_2$ decreases, due to less oxidation of CO into CO_2.

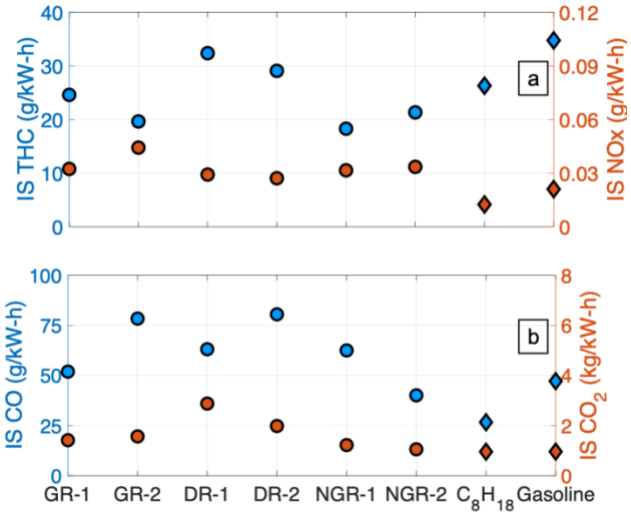

Figure 18: a) Indicated specific THC and NOx emissions, and b) indicated specific CO and CO_2 emissions

The reactivity of the all the six reformate fuels were studied in detail at a compression ratio of 16 and equivalence ratio of 0.31 at a constant CA50. Their autoignition characteristics can be

characterized using a predeveloped PRF mapping [48]. The PRF number/octane rating mapping was conducted on the same CFR engine and at the same equivalence ratio, engine speed, and CA50 as the experiments in this paper. The PRF mapping used PRF blends from PRF 0 to PRF 100. The combustion phasing was maintained constant by changing the intake temperature, between 300K and 400K, and by changing the compression ratio, between 8 to 16. Since all of the reformate fuels were tested at a compression ratio of 16, all of the possible PRF blends at that compression ratio were chosen for comparisons, along with gasoline and natural gas at the same compression ratio. As the octane rating of these fuels are known, a trend line relating intake temperature and effective octane rating can be generated. Knowing the intake temperature requirement of the reformate fuels at the same equivalence ratio and combustion phasing, their effective PRF number or effective octane number can be determined and is presented in the Figure 19. All of the gaseous reformate fuel mixtures had an effective octane rating for LTC of between 102 and 117.

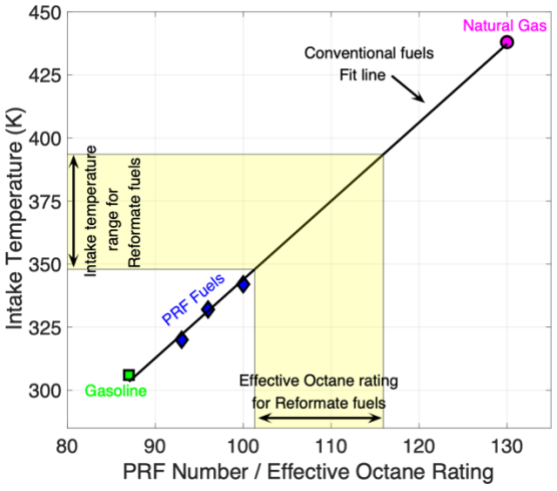

Figure 19: Characterization of reformate fuel effective octane rating in LTC

Conclusions:

In this study, three parent fuels, gasoline, diesel, and natural gas, underwent catalytic partial oxidation to form gaseous reformate fuel mixtures. Reformation was conducted at both a high and a low pressure, at numerous equivalence ratios. The composition of the reformation products and the energy released during reformation are then compared. The following key results were found:

1. For natural gas, methane conversion during reformation at low-pressure is higher than at high-pressure. H_2 and CO formation are inversely proportional to the equivalence ratio. The energy released in natural gas reformation decreases as equivalence ratio increases.

2. During the low-pressure reformation, oxidation of gasoline is inversely proportional to the equivalence ratio. During the high-pressure reformation, oxidation of gasoline is near constant. The energy released during the low-pressure reformation of gasoline increases as equivalence ratio decreases.

3. The oxidation of diesel is constant, regardless of equivalence ratio or pressure. This results in a relatively constant fraction of energy released during reformation, irrespective of pressure and equivalence ratio, possibly due to the low temperature chemistry of diesel fuel.

Two reformate fuels were then selected for each parent fuel, and their combustion characteristics were tested in a CFR engine in HCCI combustion. The following conclusions can be drawn from these experiments:

1. The lower heating value of each selected reformate fuel was significantly lower than their parent fuel due to the diluents associated with a CPOX process (N_2, CO_2, and H_2O). These diluents then affected the peak bulk temperature, NO_x, and CO emissions consistent with the known trends of LTC.

2. In both the gasoline and diesel reformates, the peak heat release rate increases when a fraction of N_2 concentration in the reformate fuel is replaced by CO. The required intake temperature subsequently decreased to maintain the combustion phasing.

3. However, in the natural gas reformates, when a fraction of N_2 is replaced by CH_4, the required intake temperature increased due to the high-octane rating of methane.

4. Unlike some of the parent fuels, none of the reformate fuels show any low- or intermediate-temperature heat release. Instead, they all underwent single-stage heat release.

5. The effective octane rating of the six reformate fuels was determined by their intake temperature requirement to achieve autoignition. They were all similar and they all were slightly harder to autoignite than gasoline or iso-octane, but significantly easier than natural gas.

Acknowledgements

The authors wish to gratefully acknowledge the financial support of the Department of Energy under award number DE-EE0007216.

Abbreviations:

ATR	Autothermal Reforming
BDC	Bottom Dead Center
CA50	Crank angle at which 50% of the fuel is burned
CFR	CoOperative Fuel Research
CoV	Coefficient of Variance
CPOX	Catalytic Partial Oxidation
D-EGR	Dedicated - EGR
EGR	Exhaust Gas Recirculation
EHN	Ethyl-Hexyl Nitrate
EI	Emission Index
GC	Gas Chromatograph
HCCI	Homogeneous Charge Compression Ignition
IMEPn	Net Indicated Mean Effective Pressure
LHV	Lower Heating Value
LTC	Low Temperature Combustion
MEXA	Motor Exhaust Gas Analyzer
MPRR	Maximum Pressure Rise Rate
NVO	Negative Valve Overlap
PCCI	Premixed Charge Compression Ignition
PRF	Primary Reference Fuel
RCCI	Reactivity Controlled Compression Ignition
SI	Spark Ignition
SR	Steam Reforming
TDC	Top Dead Center

Appendix:

Table A 1 : Complete concentration of the product of reformation process

Fuel Name	**GR-1**	**GR-2**		**DR-1**	**DR-2**		**NGR-1**	**NGR-2**
Equivalence Ratio	5.2	4.8		4.17	3.67		6	3.75
Components								
H_2	7.59%	9.79%	H_2	2.56%	4.87%	H_2	21.02%	20.87%
O_2	0.32%	0.08%	O_2	0.21%	0.03%	O_2	1.08%	2.51%
N_2	55.70%	55.02%	N_2	65.46%	62.27%	N_2	39.75%	48.46%
CH_4	3.47%	3.70%	CH_4	1.14%	2.06%	CH_4	20.37%	8.42%
CO	5.84%	14.98%	CO	2.86%	7.18%	CO	10.53%	11.04%
CO_2	4.59%	3.90%	CO_2	9.32%	7.40%	CO_2	3.19%	3.40%
C_2H_4	3.56%	3.28%	C_2H_4	2.44%	2.96%			
C_2H_6	0.26%	0.21%	C_2H_6	0.17%	0.19%	C_2H_6	0.01%	0.01%
C_2H_2	0.13%	0.18%	C_2H_2	0.04%	0.17%			
CH_2O	0.00%	0.00%	CH_2O	0.00%	0.00%			
C_3H_4	0.02%	0.02%	C_3H_4	0.00%	0.00%			
C_2H_4O	0.01%	0.00%	C_2H_4O	0.00%	0.00%			
C_3H_6	0.42%	0.19%	C_3H_6	0.04%	0.02%			
C_3H_8	0.01%	0.00%	C_3H_8	0.00%	0.00%			
Gasoline	3.57%	1.75%	Diesel	2.53%	1.47%			
H_2O	14.44%	6.91%	H_2O	13.21%	11.40%	H_2O	4.05%	5.29%

Table A 2 : Operating conditions for the reformate fuels and their combustion characteristics

		Gasoline Reformates		Diesel Reformates		Natural Gas Reformates	
		GR-1	GR-2	DR-1	DR-2	NGR-1	NGR-2
Equivalence ratio		0.31	0.30	0.32	0.30	0.30	0.32
IMEPn (bar)		2.17	2.22	1.99	2.09	1.89	1.89
LHV (MJ/kg)		4.227	5.330	1.772	2.884	5.978	10.209
Fuel Density (kg/m^3)		1.073	1.060	1.193	1.145	0.892	0.844
Stoichiometric AFR		1.626	1.766	0.707	1.127	2.206	4.008
Mass of air (g/cycle)		0.412	0.420	0.294	0.371	0.425	0.432
Mass of fuel (g/cycle)		0.089	0.072	0.197	0.126	0.057	0.035
CA50		4.4	3.8	4.0	4.3	4.6	3.8
CA25to75		3.5	3.2	3.8	3.8	4.1	3.6
CA10to90		6.8	6.3	7.4	7.6	8.3	7.2
Start of combustion (deg aTDC)		-3.20	-3.40	-4.00	-3.60	-3.40	-4.20
Intake temperature (K)		357.1	347.9	372.3	351.9	361.0	393.5
Exhaust temperature (K)		537.2	544.2	536.4	537.5	531.4	538.1
Peak bulk temperature (K)		1416.1	1439.0	1408.3	1383.4	1346.7	1442.6
Bulk temperature at start of combustion (K)		894.7	899.7	903.1	892.0	894.9	934.6
Energy in (J)		336.6	344.8	318.1	319.9	305.6	315.8
Cumulative heat transfer (J)		75.4	80.8	75.0	70.6	74.9	81.3
MPRR (bar/CAD)		3.1	3.6	2.6	2.7	2.5	2.8
Efficiency	Thermal (%)	43.5	43.4	42.4	43.7	42.2	40.9
	Combustion (%)	89.18	89.25	91.30	88.14	88.98	88.98
Indicated Specific	CO (g/kW-h)	51.9	78.4	63.1	80.5	62.5	40.1
	CO_2 (kg/kW-h)	1.42	1.57	2.88	1.99	1.23	1.06
	THC (g/kW-h)	24.6	19.7	32.4	29.1	18.3	21.3
	NOx (g/kW-h)	0.03	0.04	0.03	0.03	0.03	0.03

References:

1. Walker, N. R., Chuahy, F. D., & Reitz, R. D. (2015, November). Comparison of diesel pilot ignition (DPI) and reactivity controlled compression ignition (RCCI) in a heavy-duty engine. In ASME 2015 Internal Combustion Engine Division Fall Technical Conference (pp. V001T03A016-V001T03A016). American Society of Mechanical Engineers.
2. Wissink, M., & Reitz, R. D. (2015). Direct dual fuel stratification, a path to combine the benefits of RCCI and PPC. SAE International Journal of Engines, 8(2), 878-889.
3. Kokjohn, S., Hanson, R., Splitter, D., Kaddatz, J., & Reitz, R. (2011). Fuel reactivity controlled compression ignition (RCCI) combustion in light-and heavy-duty engines. SAE International Journal of Engines, 4(1), 360-374.
4. Noehre, C., Andersson, M., Johansson, B., & Hultqvist, A. (2006). Characterization of partially premixed combustion (No. 2006-01-3412). SAE Technical Paper.
5. Han, D., Ickes, A. M., Bohac, S. V., Huang, Z., & Assanis, D. N. (2011). Premixed low-temperature combustion of blends of diesel and gasoline in a high speed compression ignition engine. Proceedings of the Combustion Institute, 33(2), 3039-3046.
6. Dec, J. E., Yang, Y., & Dronniou, N. (2011). Boosted HCCI-controlling pressure-rise rates for performance improvements using partial fuel stratification with conventional gasoline. SAE International Journal of Engines, 4(1), 1169-1189.
7. Hwang, W., Dec, J., & Sjöberg, M. (2008). Spectroscopic and chemical-kinetic analysis of the phases of HCCI autoignition and combustion for single-and two-stage ignition fuels. Combustion and Flame, 154(3), 387-409.
8. Hanson, R. M., Kokjohn, S. L., Splitter, D. A., & Reitz, R. D. (2010). An experimental investigation of fuel reactivity controlled PCCI combustion in a heavy-duty engine. SAE international journal of engines, 3(1), 700-716.
9. D.F. Chuahy, F., & Kokjohn, S. L. (2017). Effects of reformed fuel composition in “single” fuel reactivity controlled compression ignition combustion. Applied Energy, 208, 1–11. doi:10.1016/j.apenergy.2017.10.057
10. Luong, M. B., Yu, G. H., Chung, S. H., & Yoo, C. S. (2017). Ignition of a lean PRF/air mixture under RCCI/SCCI conditions: Chemical aspects. Proceedings of the Combustion Institute, 36(3), 3587-3596.
11. Splitter, D., Reitz, R., & Hanson, R. (2010). High efficiency, low emissions RCCI combustion by use of a fuel additive. SAE International Journal of Fuels and Lubricants, 3(2), 742-756.
12. Bornemann, H., Scheidt, F., & Sander, W. (2002). Thermal decomposition of 2-ethylhexyl nitrate (2-EHN). International journal of chemical kinetics, 34(1), 34-38.
13. Dempsey, A., Curran, S., and Reitz, R., "Characterization of Reactivity Controlled Compression Ignition (RCCI) Using Premixed Gasoline and Direct-Injected Gasoline with a Cetane Improver on a Multi-Cylinder Engine," SAE Int. J. Engines 8(2):859-877, 2015, https://doi.org/10.4271/2015-01-0855.
14. Ickes, A. M., Bohac, S. V., & Assanis, D. N. (2009). Effect of 2-ethylhexyl nitrate cetane improver on NO x emissions from premixed low-temperature diesel combustion. Energy & Fuels, 23(10), 4943-4948.
15. Lawler, B., & Mamalis, S. (2018). U.S. Patent Application No. 15/082,469.
16. Geng, C., Liu, H., Cui, Y., Yang, Z., Fang, X., Feng, L., & Yao, M. (2019). Study on single-fuel reactivity controlled compression ignition combustion through low temperature reforming. Combustion and Flame, 199, 429-440.
17. Golunski, S. (2010). What is the point of on-board fuel reforming?. Energy & Environmental Science, 3(12), 1918-1923.

18. Tsolakis, A., Megaritis, A., & Wyszynski, M. L. (2003). Application of exhaust gas fuel reforming in compression ignition engines fueled by diesel and biodiesel fuel mixtures. Energy & fuels, 17(6), 1464-1473.
19. Tsolakis, A., Megaritis, A., & Wyszynski, M. L. (2004). Low temperature exhaust gas fuel reforming of diesel fuel. Fuel, 83(13), 1837-1845.
20. Tsolakis, A., Megaritis, A., Yap, D., & Abu-Jrai, A. (2005). Combustion characteristics and exhaust gas emissions of a diesel engine supplied with reformed EGR (No. 2005-01-2087). SAE Technical Paper.
21. Chadwell, C., Alger, T., Zuehl, J., and Gukelberger, R., "A Demonstration of Dedicated EGR on a 2.0 L GDI Engine," SAE Int. J. Engines 7(1):434-447, 2014, https://doi.org/10.4271/2014-01-1190.
22. Alger, T. and Mangold, B., "Dedicated EGR: A New Concept in High Efficiency Engines," SAE Int. J. Engines 2(1):620-631, 2009, https://doi.org/10.4271/2009-01-0694.
23. Ekoto IW, Wolk BM, Northrop WF, Hansen N, Moshammer K. Tailoring Charge Reactivity Using In-Cylinder Generated Reformate for Gasoline Compression Ignition Strategies. ASME. Internal Combustion Engine Division Fall Technical Conference, ASME 2016 Internal Combustion Engine Division Fall Technical Conference ():V001T03A019. doi:10.1115/ICEF2016-9458.
24. Peterson, B., Ekoto, I., and Northrop, W., "Investigation of Negative Valve Overlap Reforming Products Using Gas Sampling and Single-Zone Modeling," SAE Int. J. Engines 8(2):747-757, 2015, https://doi.org/10.4271/2015-01-0818
25. Kane, S., Li, X., Wolk, B., Ekoto, I. et al., "Investigation of Species from Negative Valve Overlap Reforming Using a Stochastic Reactor Model," SAE Technical Paper 2017-01-0529, 2017, https://doi.org/10.4271/2017-01-0529.
26. Wolk, B., Ekoto, I., and Northrop, W., "Investigation of Fuel Effects on In-Cylinder Reforming Chemistry Using Gas Chromatography," SAE Int. J. Engines9(2):964-978, 2016, https://doi.org/10.4271/2016-01-0753.
27. Urushihara, T., Hiraya, K., Kakuhou, A., and Itoh, T., "Expansion of HCCI Operating Region by the Combination of Direct Fuel Injection, Negative Valve Overlap and Internal Fuel Reformation," SAE Technical Paper 2003-01-0749, 2003, https://doi.org/10.4271/2003-01-0749.
28. Xu, X., Li, P., & Shen, Y. (2013). Small-scale reforming of diesel and jet fuels to make hydrogen and syngas for fuel cells: A review. Applied energy, 108, 202-217.
29. Wierzbicki, T. A., Lee, I. C., & Gupta, A. K. (2016). Recent advances in catalytic oxidation and reformation of jet fuels. Applied Energy, 165, 904-918.
30. Lyubovsky, M., Smith, L. L., Castaldi, M., Karim, H., Nentwick, B., Etemad, S., ... & Pfefferle, W. C. (2003). Catalytic combustion over platinum group catalysts: fuel-lean versus fuel-rich operation. Catalysis Today, 83(1-4), 71-84.
31. Smith, L. L., Karim, H., Castaldi, M. J., Etemad, S., & Pfefferle, W. C. (2006). Rich-catalytic lean-burn combustion for fuel-flexible operation with ultra low emissions. Catalysis Today, 117(4), 438-446.
32. Ahmed, S., & Krumpelt, M. (2001). Hydrogen from hydrocarbon fuels for fuel cells. International journal of hydrogen energy, 26(4), 291-301.
33. Edwards, N., Ellis, S. R., Frost, J. C., Golunski, S. E., van Keulen, A. N., Lindewald, N. G., & Reinkingh, J. G. (1998). On-board hydrogen generation for transport applications: the HotSpot™ methanol processor. Journal of power sources, 71(1-2), 123-128.
34. Ahmed, S., Lee, S. H., Carter, J. D., & Krumpelt, M. (2004). U.S. Patent No. 6,713,040. Washington, DC: U.S. Patent and Trademark Office.

35. Roychoudhury, S., Lyubovsky, M., Walsh, D., Chu, D., & Kallio, E. (2006). Design and development of a diesel and JP-8 logistic fuel processor. Journal of Power Sources, 160(1), 510-513.
36. Lyubovsky, M., Roychoudhury, S., & LaPierre, R. (2005). Catalytic partial "oxidation of methane to syngas" at elevated pressures. Catalysis letters, 99(3-4), 113-117.
37. Liu, K., Song, C., & Subramani, V. (2009). Hydrogen and syngas production and purification technologies. John Wiley & Sons.
38. Ma, L., Trimm, D. L., & Jiang, C. (1996). The design and testing of an autothermal reactor for the conversion of light hydrocarbons to hydrogen I. The kinetics of the catalytic oxidation of light hydrocarbons. Applied Catalysis A: General, 138(2), 275-283.
39. Kang, I., Bae, J., Yoon, S., & Yoo, Y. (2007). Performance improvement of diesel autothermal reformer by applying ultrasonic injector for effective fuel delivery. Journal of Power Sources, 172(2), 845-852.
40. Borup, R. L., Inbody, M. A., Semelsberger, T. A., Tafoya, J. I., & Guidry, D. R. (2005). Fuel composition effects on transportation fuel cell reforming. Catalysis today, 99(3-4), 263-270.
41. Karatzas, X., Nilsson, M., Dawody, J., Lindström, B., & Pettersson, L. J. (2010). Characterization and optimization of an autothermal diesel and jet fuel reformer for 5 kWe mobile fuel cell applications. Chemical Engineering Journal, 156(2), 366-379.
42. Breshears, R., Cotrill, H., & Rupe, J. (1973). Partial Hydrogen Injection into Internal Combustion Engines–Effect on Emis-sions and Fuel Economy. First Syraposium on Low Pollution Power Systems Development, Ann Arbor, Michigan.
43. Houseman, J., & Hoehn, F. W. (1974). A two-charge engine concept: hydrogen enrichment (No. 741169). SAE Technical Paper.
44. Bell, S. R., & Gupta, M. (1997). Extension of the lean operating limit for natural gas fueling of a spark ignited engine using hydrogen blending. Combustion Science and Technology, 123(1-6), 23-48.
45. Lynch, F. E., & Marmaro, R. W. (1992). U.S. Patent No. 5,139,002. Washington, DC: U.S. Patent and Trademark Office.
46. Bromberg, L., Cohn, D. R., Rabinovich, A., & Heywood, J. (2001). Emissions reductions using hydrogen from plasmatron fuel converters. International Journal of Hydrogen Energy, 26(10), 1115-1121.
47. Sandia National Laboratory's website, http://www.ca.sandia.gov/CRF
48. Yang, R., Hariharan, D., Zilg, S., Lawler, B. et al., "Efficiency and Emissions Characteristics of an HCCI Engine Fueled by Primary Reference Fuels," SAE Technical Paper 2018-01-1255, 2018, https://doi.org/10.4271/2018-01-1255.
49. Puranam, S. V., & Steeper, R. R. (2012). The Effect of Acetylene on Iso-octane Combustion in an HCCI Engine with NVO. SAE International Journal of Engines, 5(2012-01-1574), 1551-1560.
50. Chang, J., Güralp, O., Filipi, Z., Assanis, D. N., Kuo, T. W., Najt, P., & Rask, R. (2004). New heat transfer correlation for an HCCI engine derived from measurements of instantaneous surface heat flux (No. 2004-01-2996). SAE Technical paper.
51. Hu, Y., Naito, S., Kobayashi, N., & Hasatani, M. (2000). CO2, NOx and SO2 emissions from the combustion of coal with high oxygen concentration gases. Fuel, 79(15), 1925-1932.
52. Sjöberg, Magnus, and John E Dec. "An Investigation into Lowest Acceptable Combustion Temperatures for Hydrocarbon Fuels in Hcci Engines." Proceedings of the Combustion Institute 30, no. 2 (2005): 2719-26.